NONINTRUSIVE SHAFT SPEED SENSOR

S. Barkhoudarian, L. Wyett
and J. Maram

Rockwell International/Rocketdyne Division
Canoga Park, California

Abstract

A computerized literature search on nonintrusive/noncontacting speed sensing technologies was performed, resulting in 550 abstracts and 42 articles. Fourteen techniques were identified and theoretically analyzed, resulting in the recommendation of the Microwave, Infrared, and Magnetic technologies for experimental evaluation.

Test results with a novel magnetic approach, consisting of a permanent magnet placed on the rotating shaft and a pickup coil placed on the housing, indicated detection of a strong signal (25 mV) from 3.5 inches at the lowest required speed (500 rpm).

Introduction

Reusable rocket engines such as the Space Shuttle Main Engines (SSME), the Orbital Transfer Vehicles (OTV), etc., have throttling capabilities that require real-time, closed-loop control systems of engine propellant flows, combustion temperatures and pressures, and turbopump rotary speeds. In the case of the SSME, there are four turbopumps that require real-time measurement and control of their rotary speeds. Variable-reluctance magnetic speed sensors were designed, fabricated, and tested for all four turbopumps, resulting in the successful implementation and operation of three of these speed sensors during each of the 12 Shuttle flights. The fourth speed sensor, shown in Fig. 1, used in the High Pressure Oxidizer Turbopump (HPOTP), shown in Fig. 2, was removed due to structural weaknesses of its 3.5-inch long intrusive probe

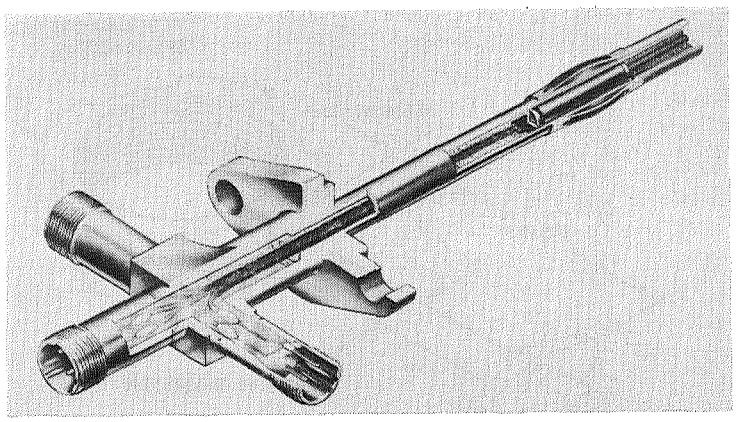

Fig. 1. High-Pressure Oxidizer Turbopump Speed Sensor

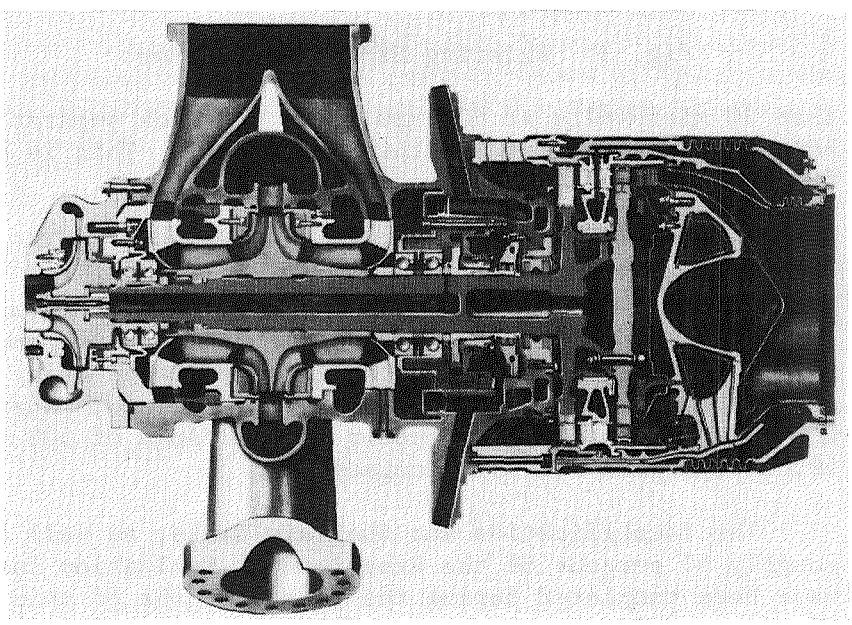

Fig. 2. High-Pressure Oxidizer Turbopump

tip, which had to withstand 200 ft/sec flow forces and 34.5 grms vibration in a liquid-oxygen environment, where loose-part collisions can ignite the propellant and have catastrophic consequences. The probe tip, shown in Fig. 3, could not have been shortened because the signal amplitude would have been reduced to less

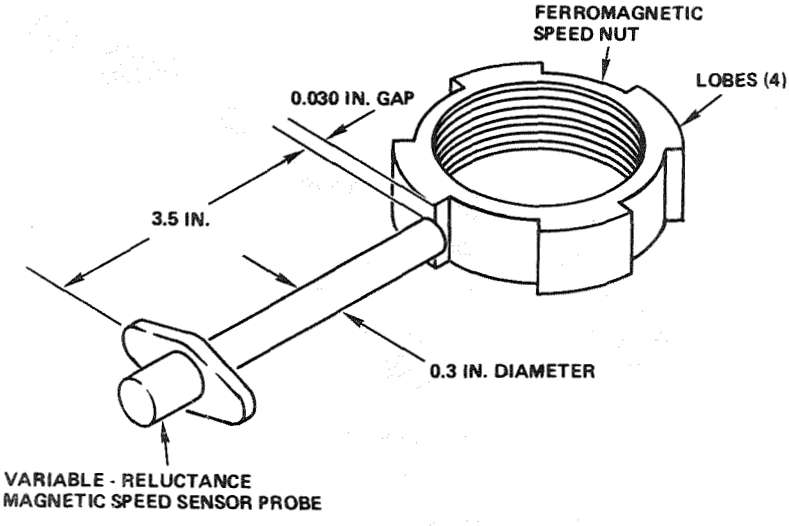

Fig. 3. Existing SSME Speed Sensor

than 20 microvolts at 500 rpm for a 3.5-inch separation between the speed nut and the pickup coil. This is an impractical signal value for SSME applications.

To overcome this problem, a technology program was initiated by MSFC resulting in a contract award to Rocketdyne. This program consists of identification, analysis, experimental evaluation of nonintrusive speed measurement techniques, and preliminary design of a selected nonintrusive speed sensor capable of measuring the speed of any SSME turbopump in the range of 500 to 50,000 rpm with ±25 rpm accuracy.

The Identification and Analysis Tasks, as well as roughly 60 percent of the Experimental Evaluation Task, have been completed during the past 8 months of this 12-month program.

Identification and Description

To identify all nonintrusive speed sensing technologies, computerized literature searches were performed to identify published articles citing keywords such as "remote," "nonintrusive," "speed," "sensor," and "measurement." These searches yielded 550 abstracts

from which 42 articles were obtained for review, resulting in 6 new technologies in addition to 8 technologies already known to us, as shown in Fig. 4.

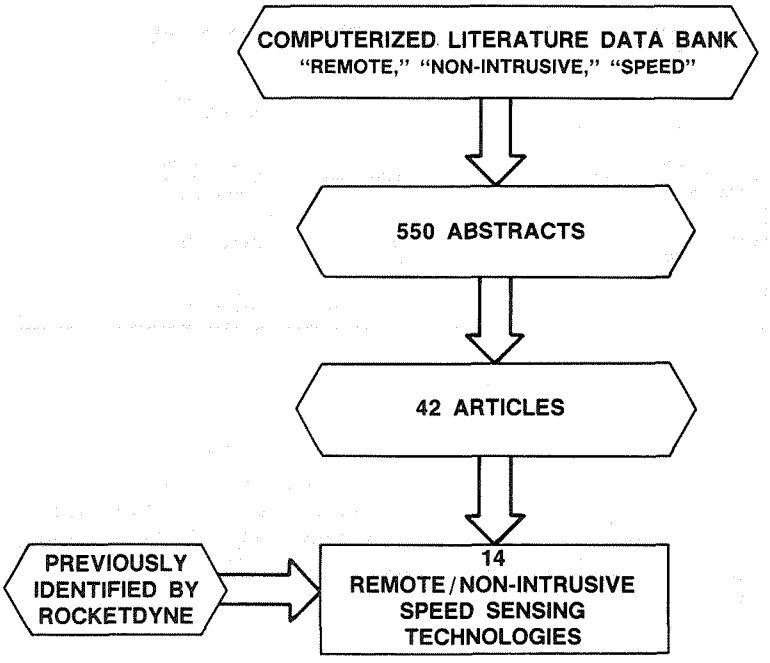

Fig. 4. Literature Search

These 14 candidate remote/nonintrusive speed sensing technologies, as shown in Table 1, were subjected to the subsequent theoretical and/or experimental evaluation. Each of the 14 technologies is briefly described below.

Capacitive Speed Sensor

A capacitive speed sensor consists of a conducting plate located at the pump housing wall and a conducting speed nut. It detects the varying capacitance due to variation in the separation between the plate and the rotating lobed speed nut and determines the shaft rotation speed from the repetition rate of these signals.

Table 1. Candidate Remote/Nonintrusive Speed (Sensing Technologies)

TECHNOLOGY	ANALYSIS APPROACH	CRITICAL PARAMETER
VARIABLE-SOURCE MAGNETIC HALL-EFFECT WIEGAND-EFFECT	MAGNETICS	LOW-RPM SIGNAL AMPLITUDE
INFRARED MICROWAVE AMPLITUDE MODULATION ELECTROMAGNETIC DOPPLER SHIFT	ELECTROMAGNETIC WAVE THEORY	CAVITATION/BUBBLE ATTENUATION
ACCELEROMETER FIBEROPTIC PROXIMETER PRESSURE PULSATION ACOUSTIC	FAST FOURIER TRANSFORMS	INTERMITTENCE, LOW-RPM SIGNAL AMPLITUDE:
CAPACITANCE EDDY CURRENT ELECTROMAGNETOACOUSTIC	LUMPED ELECTRICAL CIRCUIT ELEMENTS	AMPLITUDE SENSITIVITY
ISOTOPE	ISOTOPES	HIGH-RPM ACCURACY

Eddy Current Speed Sensor

An eddy-current speed sensor consists of an energized coil at the port and a lobed conductive speed nut on the rotating shaft. The variation in their spacing generates a periodic signal in the coil. This signal could be processed to provide a measurement of shaft speed by measuring the repetition rate of these signals.

Electromagnetoacoustic Speed Sensor

An electromagnetoacoustic speed sensor consists of an array of closely spaced permanent magnets and an eddy-current induction coil. The coil, when excited with high-frequency a-c energy, induces eddy currents in the nearby metallic lobed speed nut. The permanent magnet array, combined with the induced current, generates in the speed nut an array of alternating force zones that creates an acoustic signal. Another similar transducer, acting as a receiver, generates a periodic electrical signal due to the varying separation between the detector and the speed nut. The repetition rate of the amplitude modulated signal can be processed to provide the measurement of the shaft speed.

Fiberoptic Proximeter Speed Sensor

A fiberoptic deflectometer consists of a fiberoptic proximity detection instrument that is inserted

through a bearing housing to detect the deflection of the external surface of the bearing's outer race due to rolling balls. The fiberoptic deflectometer output signal could be processed by a Fast Fourier Transform analyzer to provide frequency information for speed measurement purposes.

Accelerometer Speed Sensor

In this approach, piezoelectric accelerometers convert turbopump-housing structural vibrations into electrical signals. For speed measurement, the signals would be processed by a Fast Fourier Transform analyzer to extract frequency information for speed measurement purposes.

Pressure Pulsation Speed Sensor

In this approach, periodic fluctuations in turbopump pressure are measured by pressure transducers and processed by a Fast Fourier Transform analyzer to extract rotational shaft speed.

Acoustic Speed Sensor

An acoustic speed sensor consists of a piezoelectric transducer emitting ultrasonic energy to a lobed speed nut, another piezoelectric transducer receiving the reflected ultrasonic energy, and an electronic system capable of processing the periodic signal whose repetition rate is proportional to the shaft speed.

Isotope Speed Sensor

An isotope speed sensor consists of a radioisotope source mounted on the speed nut and a high-energy photon detector placed on the outside of the housing. The high-energy, gamma-ray photons are detected once each time the shaft rotates and the time between successive photon bursts is measured to determine the shaft rotation speed.

Variable-Source Magnetic Speed Sensor

A variable-source magnetic speed sensor utilizes shaft-mounted, rare-earth magnets as flux generators and a nonintrusive, high-permeability pickup coil mounted at the speed sensor port at the outside of the housing. The periodic signal of such a sensor provides measurement of shaft speed.

Hall-Effect Speed Sensor

A Hall-effect speed sensor is similar to the variable reluctance speed sensors used on the SSME, except that solid-state, Hall-effect detectors are used instead of a pickup coil for detection of magnetic field variations.

Wiegand-Effect Speed Sensor

The Wiegand-effect speed sensor is similar to the variable reluctance speed sensor except that a Wiegand-effect core is used instead of a magnetically soft core for the pickup coil to generate a constant-amplitude signal. Such a speed sensor is presently used in commercial automotive applications.

Infrared Speed Sensor

An infrared speed sensor consists of an infrared light-emitting diode or diode laser that directs its beam toward a speed nut encoder typically consisting of alternately polished and matted surfaces. A periodic infrared signal corresponding to the passage of the encoder surfaces is reflected back to a solid-state infrared detector. The output of the detector is processed to provide a shaft speed measurement.

Microwave Speed Sensor

A microwave signal, generated by a Gunn diode, is transmitted through a hollow metal waveguide and a ceramic window to a lobed speed nut. The amplitude of

reflected microwave energy off the speed nut is collected and processed to produce a periodic signal whose repetition rate is a measure of shaft speed.

Electromagnetic Doppler Speed Sensor

The electromagnetic Doppler approach utilizes the change in frequency observed when a microwave signal is reflected from the moving speed nut. The speed of the nut is thus measured directly and continuously, unlike the microwave approach discussed above. Additionally, sharp encoder lobes are not required; the surface roughness of the existing turbopump shaft may reflect sufficient microwave energy for Doppler signal detection.

Analysis

Each of 14 technologies were theoretically analyzed to determine their compatibility with SSME turbopump hardware, performance, environment, and controller requirements. Those technologies that did not satisfy all the requirements were rejected. The remaining technologies were recommended for experimental evaluation. To facilitate the analysis, these 14 technologies are categorized according to the fundamental principles governing their performance. Thus, the capacitance, eddy-current, and electromagnetoacoustic speed-sensing technologies are grouped together because their performance can be evaluated by analyses of equivalent electrical lumped circuit components. The accelerometer, acoustic, pressure, and proximeter speed-sensing technologies are grouped together since their performance is dependent on the effectiveness of Fast Fourier Transform (FFT) analyses. The microwave, electromagnetic-Doppler, and infrared technologies are grouped together, the performance of each being affected by the propagation of electromagnetic waves through a cavitating liquid medium. The magnetic, Hall-effect and Wiegand-effect technologies are grouped together because their performance can be determined by analyses based on principles of magnetics.

Lumped-Electrical Circuit Group

This group was analyzed for sensitivity of detection using an effectively static lumped component

representing the housing, shaft, vanes, and sensor hole and an effective dynamic lumped component representing the changing gap of the speed nut periphery. All three technologies indicated a sensitivity of less than one part in ten thousand as determined from the following calculations.

The capacitance sensor configuration was simplified to represent a dynamic capacitance consisting of two port-size parallel plates separated by the distance from the port to the speed nut periphery ($C_d = \varepsilon A/g$), and by a static cylindrical capacitance [$C_s = 2\pi EL/\ell n(L/R\sqrt{3})$] generated by the sensor hole and the housing and shaft. The fractional change in total effective capacitance, $\Delta C_d/C_s$, was calculated to be less than 1×10^{-4}, which was considered to be too small for accurate measurements.

In a similar analysis, the eddy-current sensor configuration was broken down to dynamic and static mutual inductances resulting in a change in total mutual inductance of less than 2×10^{-5}, once again too small for accurate measurements.

The electromagnetoacoustic sensor, consisting of an eddy-current sensor superimposed with permanent magnets, was determined to be no more sensitive than the eddy-current sensor.

FFT Group Analysis

The feasibility of the fiberoptic proximeter, accelerometer, pressure pulsation, and acoustic speed sensing technologies was evaluated using data available from previous turbopump tests. The data were reprocessed to provide power spectral density (PSD) plots, time profiles, and isoplots, with the goal of identifying shaft speed related signals valid over the 500 to 50,000 rpm range of the turbopump. In all cases, the data indicated the presence of intermittent and unreliable signals below at least 3000 rpm rendering these approaches unacceptable to meet the SSME requirements.

The fiberoptic proximeter data revealed numerous bearing-related signals. The shaft rotation/inner race frequency, the cage frequency, the ball pass frequency, and their harmonics were identified in the bearing data. Although strong frequency trends do stand out in the data, there are many sampling periods when the signals are ambiguous and fade out completely, or are superimposed, thus making identification of the frequency component source for closed-loop measurements questionable. It was concluded that there were no readily identifiable amplitude or frequency relationships present that could be counted upon for continuous speed measurement over the duration of the tests.

The analyses of accelerometer data from previous SSME high pressure oxidizer turbopump tests has yielded readily identifiable synchronous frequencies and impeller blade-wake frequency harmonics (4x and 8x synchronous frequency) at steady-state high rpm speeds. However, the high pressure oxidizer turbopump data often contained High Pressure Fuel Turbopump (HPFTP) vibration signals, and all of the high pressure oxidizer turbopump related signals were found to have periods of intermittence during the tests. For example, no speed-related signals were found below 13,200 rpm and all synchronous frequencies below 3000 rpm were masked by noise.

Pressure pulses obtained from the SSME high pressure oxidizer turbopump high-frequency pressure sensors were responsive to changes in portions of turbopump speed ramp down (from 27,600 to 19,500 rpm) and ramp up (higher than 25,000 rpm) beyond 3 seconds after startup. The lack of reliable speed-linked pressure pulsations during all other turbopump operating conditions renders this technology unsuitable for closed-loop speed measurement over the required rpm range.

The ultrasonic vibration measurement system reported by Hamilton (cited in the Bibliography) presented test results of a small (1/4-inch diameter shaft) universal motor, but did not include any power spectral density curves of the output signal. It is our opinion that such an analysis would have produced power spectral

density plots similar to the ones obtained from fiber-optic deflectometer, accelerometer, and pressure pulsation measurements and followed, therefore, their destiny: the signal is intermittent, weak, and unreliable at low speeds. Therefore, this acoustic technology was also removed from consideration for experimental evaluation.

Isotope Speed Sensor Analysis

An analysis was performed to determine the total photon count at the isotope speed sensor detector and the relationship between the isotope source strength and the accuracy of speed measurement. For simplicity, it was assumed that the total photon count is proportional to source strength, solid angle of capture, absorption losses, detector efficiency, rotation period, multiplicity of isotope decay, and viewing angle. Specifically, it was assumed that the source had 5 millicurie strength, a decay multiplicity of 2, 1.1 MeV energy, a 1 percent solid angle capture, and is placed 2.7 inches away from an 80-percent efficient detector. With the above assumptions, a total photon count of only 2 was calculated at 30,000 rpm, which implies a 70-percent scatter (equivalent to one standard deviation) in measurement.

To approach a ±25 rpm accuracy, 4 million counts are required, indicating that the isotope approach would require an extremely high strength source which would not be NRC-exempt, rendering it impractical.

Magnetic Group Analysis

An analysis was performed to determine the amplitude of the signal generated in a pickup coil by the rotating permanent magnet in the variable-source magnetic speed sensor, as shown in Fig. 5. It was assumed that if a peak magnetic induction of 6 Gauss can be generated by the four shaft-mounted magnets in a pickup coil at a distance of 2 inches, then the induction at the coil would vary from 0 to 6 Gauss over the time interval required for the shaft to rotate one quarter turn. The voltage generated at the

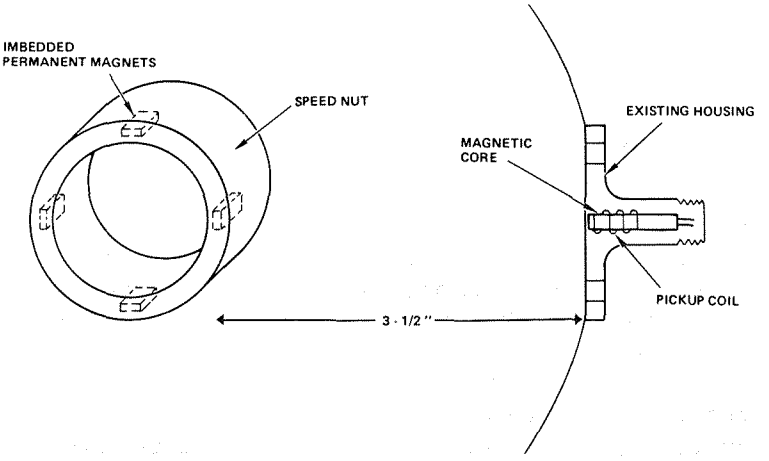

Fig. 5. Nonintrusive HPOTP Variable-Source Magnetic Speed Sensor

lowest usable SSME high pressure oxidizer turbopump speed (500 rpm) from a linear magnetic field distribution in an air-core pickup coil having 2400 turns (similar to the existing sensor coil) with a cross section equal to the existing port area was determined to be 4.7 mV, using an analysis based upon Faraday's Law. In practice, the magnetic field does not vary linearly. Rather, a much sharper flux density change over a distance approximately equal to the width of the magnet would be observed.

The analysis of Hall-effect or Weigand-effect magnetic speed sensors follows the analysis of the variable-source magnetic speed sensor except that in these approaches, the detector is not a pickup coil but is either a Hall-effect or Wiegand-effect detector. Hall-effect detectors require external excitation and so were rejected due to the possible hazard they could pose in a liquid oxygen environment. The Wiegand-effect detector generates a constant-amplitude signal due to triggering of a magnetically soft core, but requires impractically high magnetization levels for triggering and was not recommended for experimentation due to the anticipated low levels of magnetization

that would be generated in a Wiegand device by permanent magnets 3.5 inches away.

Electromagnetic Group Analysis

Both the microwave and the infrared approach to nonintrusive speed sensing must demonstrate sufficient immunity to propellant cavitation to be considered as viable technologies. An analysis was therefore performed to determine the impact of cavitation on the effectiveness of these techniques.

From the Mie theory, the transmittance, T, through a medium with nonabsorbing spherical scatters takes the form:

$$T = \exp(-N\pi R^2 QL) = \exp(-3CQL/4R)$$

where

- N = bubble concentration (cm^{-3}) = $3C/4\pi R^3$
- C = cavitation fraction (by volume)
- R = bubble radius (cm)
- L = path length (= 20 cm roundtrip)
- Q = scattering coefficient = $2-(4 \sin P)/P + 4 (1-\cos P)/P^2$
- P = $4\pi R(1-M)/\lambda$
- M = ratio of refractive indices ($n_1/n_2 = 0.8$)
- λ = wavelength (cm)

Transmittances were calculated for assumed levels of cavitation (0.1 and 1 percent) for visible, infrared, and microwave wavelengths for bubble radii on the order of the wavelength utilized. The results of the calculations are presented in Table 2. The transmittances for both 0.1 and 1.0 cm wavelength microwaves indicate that acceptable signal levels will be detected even under conditions of severe cavitation, making the

Table 2. Mie Scattering Transmittance

ENERGY FORM	WAVELENGTH	TRANSMITTANCE	
		0.001 CAVITATION	0.01 CAVITATION
MICROWAVE	1 CM	>0.85	>0.20
	0.1 CM	>0.20	$>10^{-7}$
INFRARED	30 MICRON	$<10^{-4}$	0
	5 MICRON	$<10^{-10}$	0
	1.3 MICRON	0	0
VISIBLE	0.5 MICRON	0	0

microwave approach very promising. The shorter wavelengths, however, suffer considerably from the scattering effects of oxygen bubbles in liquid oxygen. The visible wavelength (0.5 micrometer) and the shorter infrared wavelengths (1.3 and 5 micrometers) undergo several signal loss by scattering and are rendered unusable. The 30-micrometer infrared radiation offers acceptable transmittance over most of the range of bubble radii for a cavitation level of 0.1 percent, but is unacceptable for 1 percent cavitation.

Mie scattering calculations performed at the same cavitation levels, but for bubble radii in the range of 0.01 to 1.0 centimeter demonstrate sufficient transmittance (5 to 97 percent) for both the infrared and microwave approach to be usable for remote speed sensing applications.

It is prudent to understand the assumptions inherent in the scattering derivation. It is assumed that all scattered light, including that scattered at small angles, is considered to be removed from the beam. This is equivalent to saying that the detector is assumed to be a very large distance from the scatterer, thus subtending an infinitesimally small solid angle. However, a practical application of microwave and infrared speed-sensing technologies will employ detectors at finite distances, thus subtending finite solid angles. Studies of the angular distribution of scattering indicate that a large portion of the scattering occurs in the forward direction (i.e., toward the detector), suggesting that the effective throughput will be much greater than that indicated by the tabulated

Mie scattering results. This may be sufficient to bring the infrared transmission up to acceptable signal levels, making it suitable for speed-sensing applications.

Recommendations

The analysis of the 14 candidate technologies has screened from consideration (1) those approaches that fail to provide acceptable output signal level or accuracy, (2) those with intermittent or otherwise unreliable signals, and (3) those whose performance is masked by the extreme environments present in the SSME. The magnetic, microwave, and infrared technologies demonstrated promise for use in nonintrusive shaft speed sensing and were recommended for experimental evaluation. Specifically, the quantification of signal amplitude of the variable-source magnetic speed sensor at low rpm and the attenuation of microwave and infrared energy through a cavitating medium were recommended for experimental evaluation to verify the feasibility of these technologies.

Experimental Evaluation

Variable-Source Magnetic Speed Sensor Experimentation

The variable-source magnetic speed sensor was tested in the laboratory to determine the detectability of the signal at low speeds and large separations. Four 0.5-inch diameter, disk-shaped ferrite magnets with measured pole strengths ranging from 400 to 500 Gauss were epoxied to a nonmagnetic wheel having an outside diameter equal to the SSME speed nut diameter (see Fig. 3). The wheel was rotated with an electric motor at speeds of 240, 480, and 720 rpm and magnetic pulses were observed at various distances from the wheel with an SSME high pressure oxidizer turbopump speed sensor coil. The results of these tests are graphed in Fig. 6, indicating the generation of a useful signal of 0.6 mV at the lowest required speed of (480 rpm) with a 3-inch separation.

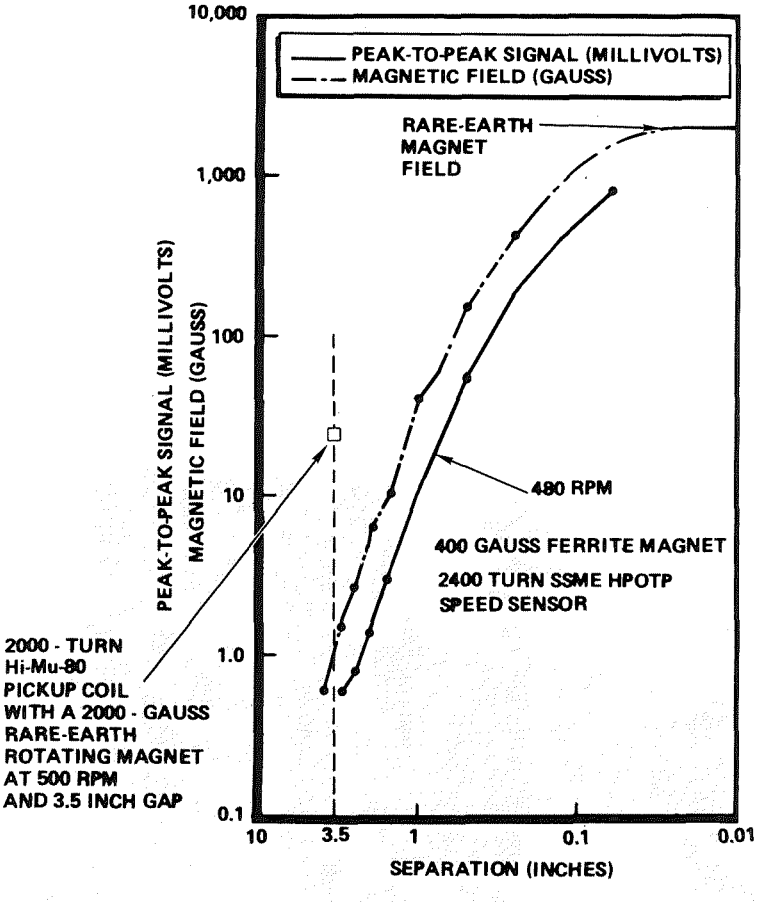

Fig. 6. Variable-Source Magnetic Speed Sensor (Electrical Signal and Field Strengths vs Separation of Magnet From Coil)

A similar test with a samarium-cobalt magnet produced a signal of 2.4 mV with the existing SSME speed sensor at a distance of 2 inches and a speed of 240 rpm. This was a threefold improvement over the signal derived from the ferrite magnet (0.8 mV at 2-inch separation). Further signal enhancement was obtained by using a hand-made 1000-turn pickup coil with a larger cross-sectional area (7/8 x 7/8 inch). At 240 rpm and 2 inches away, a signal of 25 mV_{p-p} was obtained from the rare-earth magnet. The signal would be approximately 27 mV_{p-p} at the minimum specified

speed of 500 rpm and 3-inch separation, representing a very strong signal for speed measurement.

Additional tests were performed at higher rpm's to determine the high-frequency shielding effect of turbine vanes and housing placed between the coil and magnets, as shown in Fig. 7. Four Ferrite magnets were next molded into an epoxy ring on a 2-inch diameter aluminum tube, which was spun over a speed range of 2000 to 6000 rpm with an existing test rig. Output pulses from a 2000-turn (7/8 x 7/8 inch) air core pickup coil were measured at a distance of 3.5 inches from the magnets, as shown in Fig. 8. Various metal plates

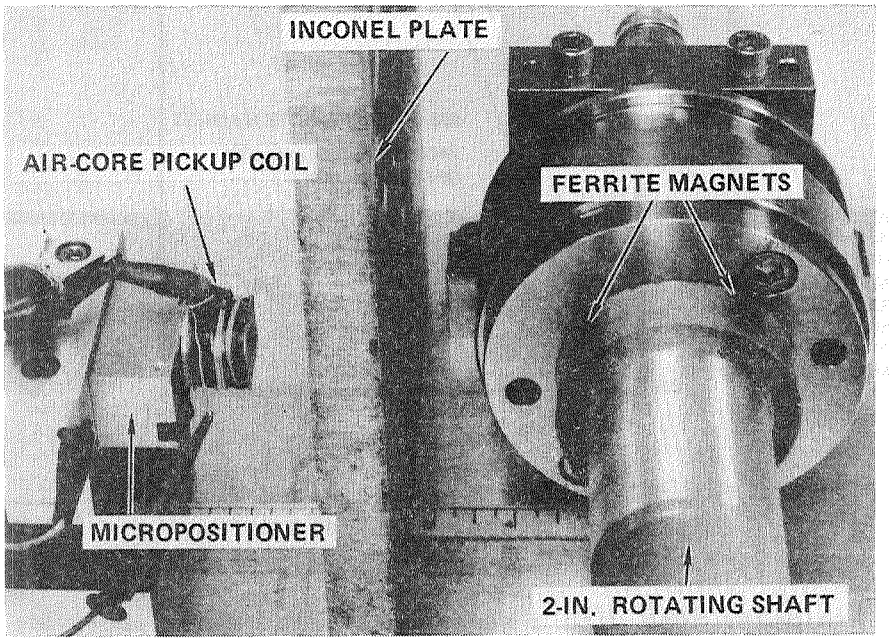

Fig. 7. Variable-Source Magnetic Speed Sensor Experimental Setup

were held tightly against the nylon spool of the pickup coil, simulating a housing-mounted coil as shown in Fig. 5. The results of the shielding of these plates are shown in Fig. 8, where a 1.2 x 12 x 18 inch Inconel 718 plate and 1.75 x 12 x 12 inch Inconel 625 plate did not attenuate the signal at all, yet a 0.75 x 7 x 16 inch aluminum plate significantly reduced the signal.

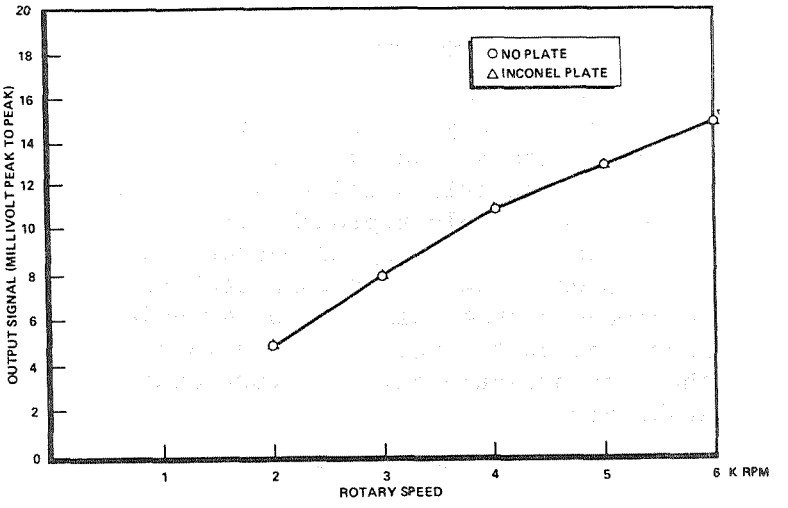

Fig. 8. Variable-Source Magnetic Speed Sensor (Signal Amplitude vs Rotating Speed)

The cause of this difference in signal reduction between aluminum and Inconel is due to the difference in electrical resistivity of the two metals. Aluminum is a very good conductor whose resistivity ranges from 1 to 3 microhm inches depending on the temperature, heat treatment, and alloy composition. The resistivity of Inconel is substantially greater than that of aluminum and ranges from 39 to 48 microhm inches even at cryogenic temperatures. Thus, eddy currents are not readily set up in Inconel, and the original magnetic field is not cancelled by its passage through Inconel.

In summary, the variable-source magnetic speed sensor, even at low speeds, can generate strong signals at a 3.5-inch distance from the speed nut, and does not lose any signal due to eddy currents in the existing intervening turbopump housing or vane materials. Thus, this sensor can be mounted completely external the turbopump housing. In view of this nonintrusiveness, and of the sensor's use of space-proven technology and its inherent immunity to bubbles and cavitation, we conclude that it is a highly viable and desirable sensor for the SSME.

Conclusions

Based upon the results of the computerized literature search, technology identification, theoretical analysis, and experimental evaluation, we conclude that the variable-source magnetic speed-sensing technology is both a viable and a desirable approach for accurate and nonintrusive turbopump shaft speed measurement. In view of its space-proven hardware and complete nonintrusiveness, it is recommended that this technology undergo immediate preliminary design for incorporation into the SSME to restore the high pressure oxidizer turbopump speed measurement capability.

Acknowledgements

This work was sponsored by NASA-MSFC under Contract NAS8-34658 with Mr. T. Marshall and H. Burke as Project Monitors. We gratefully acknowledge the support of George Kuhr and Don Hunter of Rocketdyne in the theoretical analysis and experimental verfication of the variable-source speed sensor. We would also like to thank Dr. Ira Goldberg and Dr. Jim Rode of Rockwell International/Science Center for their consultation on the experimental evaluation of the microwave and infrared speed sensors.

Bibliography

The following list of articles and reports generated as a result of the literature survey and utilized in the Theoretical Analysis, serves as a useful bibliography on the state of the art in nonintrusive speed sensors.

Anon, "Wiegand Effect: A New Pulse-Generating Option," Automotive Engineering, 86(2), February 2, 1978, pp. 44-48.

Bhartia, P. and M. A. K. Hamid, "Droppler Radar Determination of the Rotation Speed of Shafts," IEEE Trans. Ind. Electronics and Control Instrumentation, V. IECI-24, No. 1 (1977) p. 141.

Bucurenciu, S., "Dynamic Behavior of the Induction Tachometer," Rev. Roum Sci Tech Electrotech Energ 25(2) (1980) p. 149.

Gadrault, R., "Shaft Rotation Speed Measurement Device, Its Checking and Variations Checking," (U.S. Patent) February 25, 1976.

Hamilton, D. B. et al., Noncontact Devices for Measuring Vibrations and Deflections of Parts in Operating Turbopumps, Final Report, NASA CR124208.

Handlykken, M. B., "A Brushless D.C. Tachometer," (U.S. Patent) February 19, 1982.

Knoll, G. F., Radiation Detection and Measurement, Wiley, New York (1979), p. 504.

Macek, W., Electromagnetic Angular Rotation Sensing, Sperry Gyroscope Company Report, August 1964.

Noble, G. T., "Sensing Shaft Rotation With Proximity Switches," Power Transmission Des., 25(10), August 10, 1981, pp. 62-63.

Parmenov, V. I., Angular Velocity and Acceleration Pick Up, Foreign Tech. Div. Air Force Systems Command, Wright-Patterson AFB, May 26, 1964.

Transandote, A. et al., "A New Slip Monitor for Traction Equipment," Trans. of the ASAE (1977), p. 851.

Verdrunes, M. and W. E. Mace, "The Measurement of Engine Rotational Speed," AGARD Flight Test Instrumentation Series, V. 4 (1973).

Wilcox, G. and J. L. Mason, "Temperature Stabilized Tachometer for the Fuel Efficient Automobile," IEEE Trans. Consum. Electron, CE-26(3), August 3, 1980, pp. 664-669

A more detailed bibliography on nonintrusive/remote speed-sensor technologies was presented in the Nonintrusive Speed Sensor Monthly Report to NASA/MSFC for February 1984 (NASA Contract NAS8-34658).